SHORT COMMUNICATION

Electrochemical impedance of alkaline zinc/manganese dioxide cells containing no added mercury

M. J. ROOT
Rayovac Corp., PO Box 44960, Madison, Wisconsin, 53744–4960, USA

Received 16 November 1994; revised 17 February 1995

1. Introduction

Electrochemical impedance spectroscopy (EIS) has been used extensively for the characterization of a variety of electrochemical power sources targeted for consumer applications. Zinc anodes are common to many of these systems, including alkaline Zn/MnO_2 [1–6], Leclanché [4, 5, 7, 8], Zn/HgO [9] and Zn/air [10] cells.

Zinc readily corrodes in the presence of an electrolyte and in the absence of any protective additive, resulting in hydrogen gas evolution. In the worst cases, this can lead to electrolyte leakage from the cell if the internal pressure is sufficient to burst the cell seal. Until recently, mercury was added to the zinc anode to form an amalgam. This served to inhibit hydrogen evolution and decreased the contact resistance between zinc particles in cells that used powdered zinc anodes [11].

Manufacturers of electrochemical power sources have responded to environmental concerns by decreasing, or eliminating, the mercury content in certain cells containing zinc anodes. A large number of other corrosion inhibitors, usually organic compounds based on polyethylene glycol [11], have been used to reduce hydrogen evolution from zinc corrosion. The absence of mercury and the addition of organic inhibitors may be anticipated to significantly change the impedance spectra of these cells.

Previous studies on the impedance of cylindrical alkaline Zn/MnO_2 cells [1–6] were likely done with cells that used Zn(Hg) anodes. Here we report the impedance of LR6 (AA), LR14 (C) and LR20 (D) cells that contain no added mercury, but do use an organic inhibitor to suppress hydrogen gas evolution.

2. Experimental details

2.1. *Procedures*

Commercially available LR6, LR14 and LR20 cells (AA, C and D sizes, respectively) were used. In addition to obtaining complete cell impedance spectra, spectra of cell components or combinations of components were measured, following Barnard *et al.* [1], using a Hg/HgO (aqueous 38% KOH, 3% ZnO) reference electrode. A hole was carefully drilled in the side of the cell can to reveal the can–cathode interface. A Luggin–Haber reference probe containing an electrolyte gel (prepared with polyacrylic acid and an aqueous 38% KOH, 3% ZnO solution) was placed in the hole at the interface. After measuring the impedance spectrum with the can as the working electrode, a hole was drilled into the cathode to the cathode-separator interface. The reference probe was inserted to this point and the impedance spectrum of the cathode-can and separator–anode–nail combinations were measured. Finally, the bottom of the can was removed to expose the anode. The Luggin–Haber reference probe was placed at the anode-separator interface and the anode–nail spectrum was obtained. All experiments were run at ambient temperature.

To gauge the effect of an organic inhibitor on the zinc anode impedance, measurements were also done with zinc anode gels prepared in the laboratory using a polyethylene glycol–polydimethylsiloxane copolymer (DC 193) [12]. In this case, the zinc anode gels (9 M KOH, 0.5 M ZnO, polycarboxylic acid) used as both working and auxiliary electrodes were placed in copper clad metal cups (diameter = 1 cm, height = 0.5 cm) that had been galvanically plated with zinc. Zinc gels contained 0 p.p.m. or 50 p.p.m. DC 193. The Hg/HgO reference electrode used is described above.

2.2. *Equipment*

Impedance spectra were obtained with an EG&G PAR 273A potentiostat served by a Schlumberger 1255 frequency response analyser. Data were collected using EG&G model 388 software.

2.3. *Methods*

Measurements were made by superimposing a 5 mV sinusoidal voltage in the frequency range $2.5 \times 10^{-2}\ \text{Hz} \leqslant f \leqslant 1 \times 10^{5}\ \text{Hz}$ upon the open circuit potential of the cell. All reported errors are standard deviations.

3. Results and discussion

Typical complex plane impedance plots for LR6 (AA), LR14 (C) and LR20 (D) cells are given in Fig. 1. They appear qualitatively alike although impedance values inversely scale with the cell dimensions, as expected. The cell spectra are dominated by a semicircle at high frequencies and a line at low frequencies. At high frequencies ($> 1 \times 10^{3}$ to 1×10^{4} Hz), an inductance was commonly observed for this type of

0021-891X

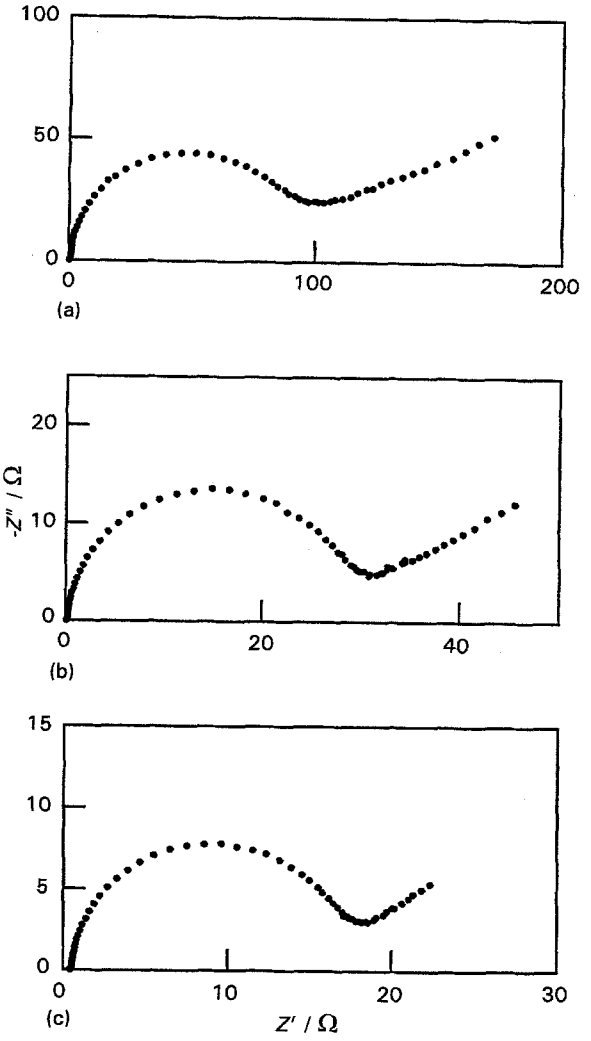

Fig. 1. Complex plane impedance plots for (a) LR6 (AA), (b) LR14 (C) and (c) LR20 (D) cells.

cell that apparently results from the various electronic contacts to the cell and within it.

Figure 2 shows the complex plane impedance plots of an LR20 (D) cell as received, the opened cell, the anode-current collector and can-cathode component combinations. Comparing plots (a) and (b) in Fig. 2, it is observed that opening the cell greatly affects its impedance. A sealed alkaline cell generally develops internal pressures greater than atmospheric pressure from hydrogen formed as the zinc slowly corrodes. The anode is a mixture of zinc powder and a gelled alkaline electrolyte prepared in such a way that it can flow. Applying pressure to this dimensionally unstable electrode may modify the interfacial electrochemistry and ohmic contacts between zinc particles. It is supposed the cathode, formed as a highly compressed powder mixture, would be less affected.

From plots (b) and (c) in Fig. 2, it may be concluded that the anode impedance is a large contributor to the cell impedance. A previous literature report [3] asserted the impedance of similar cells Zn/MnO_2 cells could be assigned to the anode. This was based on several assumptions rather than measurement of the cell component impedances, though. A correct assignment of the cell impedance was made when the

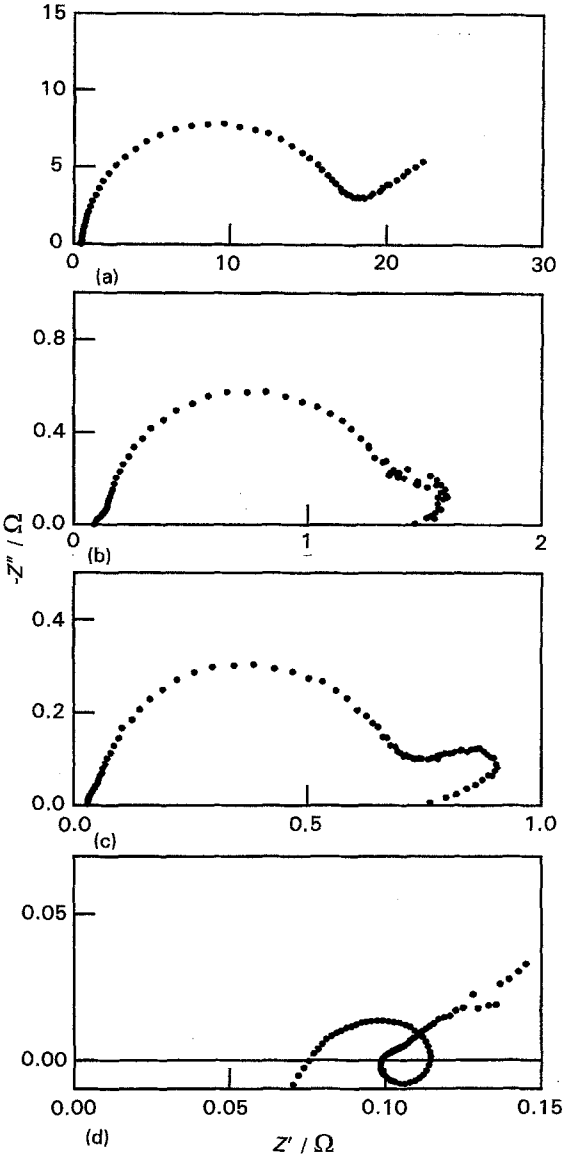

Fig. 2. Complex plane impedance plots for (a) LR20 (D) cell as received, (b) opened LR20 (D) cell, (c) anode-current collector components and (d) can-cathode components.

impedances of cell components were measured [1]. In that study it was found that the anode impedance was negligible. The cells examined in the cited works [1, 3] probably contained Zn(Hg) anodes, rather

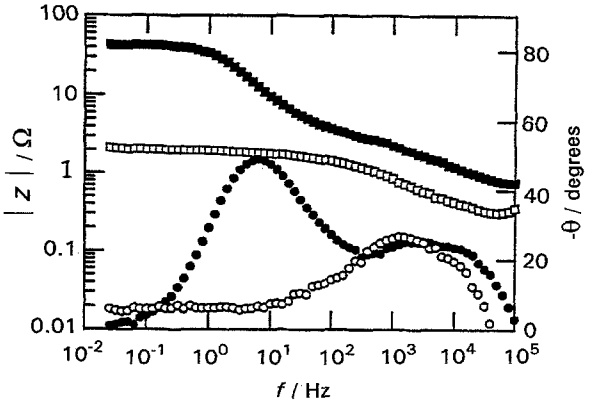

Fig. 3. Impedance magnitude, $|Z|$, and phase angle, θ, Bode plots for zinc gels (9 M KOH, 0.5 M ZnO, polycarboxylic acid): (□) 0 p.p.m. DC 193 $|Z|$; (■) 50 p.p.m. DC 193 $|Z|$; (○) 0 p.p.m. DC 193 θ; and (●) 50 p.p.m. DC 193 θ.

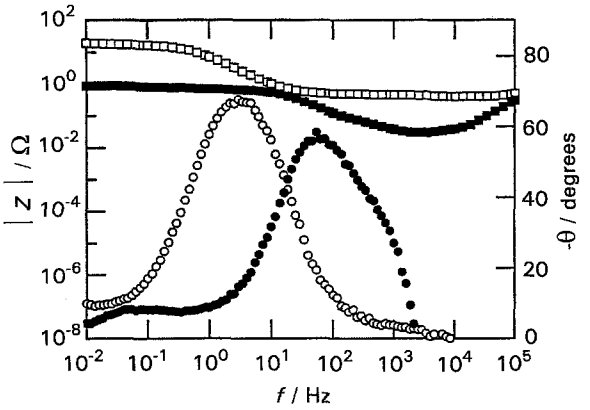

Fig. 4. Impedance magnitude, $|Z|$, and phase angle, θ, Bode plots for a LR20 (D) cell as received: (□) LR20 (D) $|Z|$; (○) LR20 (D) θ; (■) LR20 (D) anode-current collector $|Z|$; (●) LR20 (D) anode-current collector θ.

than zinc anodes without added mercury in the cells studied here. The Zn(Hg) anode is expected to have a lower impedance as a result of decreased contact resistance between zinc particles and reduced corrosion [11].

Organic corrosion inhibitors, especially polyethylene glycol and its derivatives, are typically used to reduce hydrogen evolution in the absence of mercury [11]. To assess briefly the effect of a polyethylene glycol corrosion inhibitor, the impedance spectra of zinc anode gels were measured with and without DC 193 [12]. With the addition of 50 ppm DC 193, a large semicircle appears at relatively low frequencies in the complex plane impedance plots. This change in the impedance spectrum is evident in the phase angle and impedance magnitude Bode plots (Fig. 3) near 10 Hz and apparently is a consequence of the inhibitor adsorbed on the surface of the zinc. This feature is also present in the Bode plots for the LR cells (e.g., Fig. 4), as well as their anodes, which implies that the large semicircles seen in the LR cell and anode complex plane impedance plots derive from the adsorbed inhibitor surface layer. The remainder of the anode impedance can be assigned to the electrochemical reactions of the zinc metal and transport properties within the electrolyte [13].

Using a simple parallel resistor and capacitor equivalent circuit model, calculated values of the adsorbed inhibitor surface layer capacitance and resistance are given in Table 1. The capacitance values remain relatively constant for sealed or open cells and the anode-current collector components indicating the surface layer remains largely intact. Conversely, the resistance of this layer varies widely depending on cell conditions (i.e. sealed or open). For example, resistance values of the adsorbed inhibitor layer changes from 18 Ω to 1.0 Ω to 0.70 Ω for LR20 (D) cells as received, opened cells and anode-current collector components, respectively. The decrease in adsorbed layer resistance is largely responsible for the decreased diameter of the complex plane impedance semicircle (Fig. 2) and shifts the phase angle peak in Fig. 4 to higher frequencies when the cells are opened.

As seen in Fig. 2, opening the cells dramatically alters the linear, low frequency portion of the complex plane impedance plots as well. This low frequency behaviour generally originates from transport properties within the electrode. The line curves towards the real impedance axis in the opened cells as a result of finite length diffusion [13]. While the impedance spectrum of the cathode is not likely to change much upon opening the cell [1], it is possible that changes within the anode upon opening the cell would also affect transport impedances there. Thus, it is assumed that the linear part of the complete, sealed cell spectra (Fig. 1) is from the anode.

The complex plane impedance plot of the can-cathode components in Fig. 2(d) are similar to those observed previously [1]. The semicircle is primarily a result of the can impedance [1, 15] while the exact origin of the inductive loop is unknown at this time. Low frequency linear regions of the complex plane impedance plot in Fig. 2(d) represents the cathode impedance [1, 14, 15].

4. Conclusions

Impedance measurements of individual cell components in alkaline Zn/MnO_2 electrochemical power sources have been made. These cells contain anodes with no added mercury. The spectra are dominated by the impedance characteristics of the anode. This contrasts a previous report [1] for cells that, presumably, contain Zn(Hg) anodes. In that study, it was found that the cathode was the primary source of cell impedance. Mercury acts as a corrosion inhibitor and reduces interparticle contact resistance in the anode which should act to reduce its impedance. In the absence of mercury, other corrosion inhibitors must be added to the anode. These are typically based

*Table 1. Calculated resistance and capacitance values of LR6 (AA), LR14 (C) and LR20 (D) cells as received, opened cells and anode-current collector components**

Cell size	*Cell as received*		*Cell opened*		*Anode-current collector*	
	R/Ω	$10^3\ C/F$	R/Ω	$10^3\ C/F$	R/Ω	$10^3\ C/F$
LR6 (AA)	110 ± 25	3.2 ± 0.1	5.5	3.4	1.5 ± 1.0	3.8 ± 0.6
LR14 (C)	33 ± 3.8	9.3 ± 0.2	1.1 ± 0.1	8.8 ± 1.1	1.1 ± 0.7	9.8 ± 1.4
LR20 (D)	18 ± 3.2	20 ± 0.4	1.0 ± 0.2	18 ± 1	0.70 ± 0.12	18 ± 0.1

* The uncertainties in data refer to the mean of at least two samples.

on polyethylene glycol [11]. It was found that the large semicircle in the complex plane impedance plots of the cells used here and their anodes was due to the organic corrosion inhibitor adsorbed onto the zinc surface. The low frequency linear region of the complex plane impedance plots is assigned to the anode, probably depicting transport impedance.

References

[1] R. Barnard, L. M. Baugh and C. F. Randell, *J. Appl. Electrochem.* **17** (1987) 165.
[2] *Idem, ibid.* **17** (1987) 174; 185.
[3] S. A. G. R. Karunathilaka, N. A. Hampson, R. Leek and T. J. Sinclair, *ibid.* **11** (1981) 365; 715.
[4] S. A. G. R. Karunathilaka, N. A. Hampson and R. Leek, *Surf. Technol.* **13** (1981) 339.
[5] S. A. G. R. Karunathilaka, N. A. Hampson, R. Leek and T. J. Sinclair, *J. Power Sources*, **9** (1983) 205.
[6] P. R. Roberge, M. Farahani, K. Tomantschger and E. Oran, *ibid.* **47** (1994) 13.
[7] S. A. G. R. Karunathilaka, N. A. Hampson, R. Leek and T. J. Sinclair, *J. Appl. Electrochem.* **10** (1980) 357; 603; 799.
[8] M. L. Gopikanth and S. Sathyanarayana, *ibid.* **9** (1979) 581.
[9] S. A. G. R. Karunathilaka, N. A. Hampson, T. P. Haas, R. Leek and T. J. Sinclair, *ibid.* **11** (1981) 573.
[10] V. N. Mataruev, R. T. Il'yasov, M. V. Gur'yanov and S. K. Bychkovskii, *Elektrokhim.* **27** (1991) 1057.
[11] D. Spahrbier, *Chem. Ind.* (1990) 431.
[12] R. Dopp, *US Patent 4 617 242* (1986)
[13] C. Cachet, B. Saidani and R. Wiart, *J. Electrochem. Soc.* **139** (1992) 644.
[14] B. D. Desai, F. S. Lobo and V. N. Kamat Dalal, *J. Appl. Electrochem.* **24** (1994) 917.
[15] M. J. Root, unpublished results.